Technical Note

Jets Opposing Turbidity Currents and Open Channel Flows

J. Bühler[1]; Ch. Oehy[2]; and A. J. Schleiss[3]

Abstract: Hydraulic jumps at the tail end of spillways are usually induced by baffle blocks or other obstacles. Such jumps can also be induced by jets that oppose the main flow. Another application is to back up turbidity currents in reservoirs by means of opposing jets. This measure can be adopted when transfer tunnels feed water into the reservoir at a higher elevation near the dam. Stopping the turbidity current increases the local sedimentation rate. To reconcile the shallow water equations for turbidity currents with those for open channel flows, mass-based scales for the depth and velocity of both types of flows are outlined. The continuity and momentum equation for flows opposed by jets are then stated in terms of these scales and expressed by a single curve for both gravity currents and free surface flows. The corresponding results for free surface flows agree well with those of experiments carried out for this study. An application to turbidity currents is provided as well. **DOI: 10.1061/(ASCE)HY.1943-7900.0000639.** © *2013 American Society of Civil Engineers.*

CE Database subject headings: Reservoirs; Hydraulic jump; Currents; Sediment; Jets (fluid); Open channel flow.

Author keywords: Reservoir; Hydraulic jump; Baffle block; Turbidity current; Gravity current; Sedimentation; Jet.

Introduction

Besides end sills baffle blocks are a means of stabilizing the jump at the tail end of hydraulic structures when the downstream depth is insufficient to maintain a free jump. To avoid costly maintenance of these blocks submitted to abrasion, it has been suggested that such jumps could instead be induced by water jets directed against the flow. Wilson (1977) and France (1981) conducted experiments of this type by supplying water to the jets through a duct connected to the upstream reservoir. Tople et al. (1986) determined the length and profile of these jumps. Hager (1992) contributed a state of the art review on jumps under various boundary conditions.

Jet arrangements can normally not replace end sills and baffle blocks in stilling basins as the required quantities of high pressure water are not available. Nevertheless, when opposing jets are used to stop and control turbidity currents in reservoirs the required amount of high pressure water is relatively small (Oehy et al. 2010). Alpine reservoirs are often fed by transfer tunnels bringing water to the reservoir from neighboring catchment areas. Since the transfer tunnels enter the reservoirs with a considerable height above the maximum reservoir level, they have a good potential for feeding opposing jets for controlling turbidity currents. These currents are attributable to intense rainstorms. When the resulting inflows enter a reservoir, they tend to plunge to the bottom owing to their excess density and to follow the thalweg by entraining ambient water along their path. Most of the sediment load of these underflows is eventually deposited near the dam and can impede the operation of the bottom outlets. A number of methods have been proposed for slowing down or blocking these currents and for letting them deposit their load before reaching the dam. They include the installation of permeable screens, obstacles, or bubble curtains (Oehy and Schleiss 2003). Oehy et al. (2010) reported on experiments to back up turbidity currents by means of opposing jets and showed that the sedimentation can be effectively controlled by such arrangements. The present study continues this effort by deriving the relation between upstream and downstream conditions and comparing them with experimental results. A further application of jets for removing sediments from reservoirs was proposed by Sequeiros et al. (2009).

In the first section, the traditional flow scales proposed by Ellison and Turner (1959) for the average depth, velocity, and excess density of gravity-driven underflows are outlined and compared with scales by Princevac et al. (2009, 2010). The new scales are based on the density distribution instead of the velocity distribution and are applicable for open channel flows as well. In the second section, the conservation equations for gravity currents and open channel flows opposed by jets are recast in terms of these scales. The momentum equation is solved for both cases and expressed by a single curve. In the third section, the result of this analysis is compared with experimental results for flows with a free surface, which were obtained in the laboratory of the Institute of Environmental Engineering in Zurich. In the fourth section, the results are applied to a turbidity current. Conclusions of the study are summarized at the end.

Depth and Velocity Scales for Gravity Currents

The momentum and continuity equations for jet-controlled jumps have been derived for free surface flows, but they cannot be readily applied to turbidity currents in reservoirs. The reason is that the traditional depth and velocity scales are different for the two types

[1]Senior Research Associate, Institute of Environmental Engineering, ETH Zurich, 8093 Zurich, Switzerland. E-mail: buhler@ifu.baug.ethz.ch

[2]Director, Swiss Re, Mythenquai 50/60, P.O. Box, 8022 Zurich, Switzerland; formerly, Research Assistant, Ecole Polytechnique Fédérale de Lausanne, Laboratory of Hydraulic Constructions, 1015 Lausanne, Switzerland. E-mail: Christoph_Oehy@swissre.com

[3]Professor of Hydraulic Structures, Ecole Polytechnique Fédérale de Lausanne, Laboratory of Hydraulic Constructions, Station 18, 1015 Lausanne, Switzerland (corresponding author). E-mail: anton.schleiss@epfl.ch

Note. This manuscript was submitted on July 1, 2011; approved on May 30, 2012; published online on July 23, 2012. Discussion period open until June 1, 2013; separate discussions must be submitted for individual papers. This technical note is part of the ***Journal of Hydraulic Engineering***, Vol. 139, No. 1, January 1, 2013. © ASCE, ISSN 0733-9429/2013/1-55-59/$25.00.

of flows. The depth h of flows with a free surface is the vertical extent of the dense liquid phase, and the average velocity u is derived from its flux.

A different approach was chosen by Ellison and Turner (1959) (ET) for gravity currents, in which the excess density is attributable to a stratifying agent such as heat or salt instead of sediment. On the basis of previous work on free shear flows by Morton, Taylor, and Turner (1956), they used integrals over the velocity distribution to obtain a measure for the average depth H and the streamwise velocity U of gravity currents in a calm ambient fluid. Fig. 1 shows a definition sketch for gravity currents emerging from a duct into unstratified and deep water. In the frame of reference shown in Fig. 1 it can be written

$$UH = \int \bar{u} dy$$

$$U^2 H = \int \bar{u}^2 dy$$

$$\Delta UH = B = g \int \bar{u} \frac{\bar{\rho} - \rho_a}{\rho_a} dy \tag{1}$$

where Δ = scale for the effective gravitational acceleration; and B = buoyancy flux at the source, assumed to be conserved. The overbars denote mean local values of velocity and density, and ρ_a is the density of the ambient fluid. Integrals extend from the bottom to a location in which the streamwise velocity vanishes.

The momentum equation can be stated according to ET as

$$\frac{d}{dx}\left[U^2 H + \frac{S_1}{2}\Delta H^2 \cos\varphi\right] = S_2 \Delta H \sin\varphi - C_D U^2 \tag{2}$$

where C_D = drag coefficient; and φ = slope angle. S_1 and S_2 are shape factors that relate the density distribution to these flow scales according to

$$S_1 \Delta H^2 = 2g \int \frac{\bar{\rho} - \rho_a}{\rho_a} y dy$$

$$S_2 \Delta H^2 = g \int \frac{\bar{\rho} - \rho_a}{\rho_a} dy \tag{3}$$

In the spirit of an approach by Morton, Taylor, and Turner (1956) for free shear flows, the entrainment of fluid from the upper layer was specified by an entrainment function E as

$$\frac{d}{dx}(HU) = EU \tag{4}$$

For gravity currents, E is a function of the velocity-based Richardson number $Ri_E = \Delta H \cos\varphi / U^2$. The authors also carried out experiments on saline gravity currents and determined the entrainment function E for different slopes. An important result is that the velocity U, dH/dx, and Ri_E become constant when the flow reaches an equilibrium state. An analogous transition occurs when free buoyant jets turn into plumes. For supercritical flows Princevac et al. (2009, 2010) proposed an alternative to the entrainment relation by extending a diffusion approach for jets by Prandtl (1926) and Wright (1994) to gravity currents. The diffusion and entrainment concepts agree for flows in the equilibrium state.

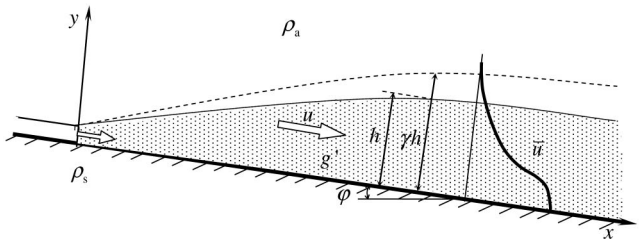

Fig. 1. Definition sketch (adapted from Princevac et al. 2010) for a gravity current (shaded region) emerging from a duct into unstratified and deep water; the mass-based flow scales are derived from the excess density distribution and the buoyancy flux; depth scales γh and h are based on the distributions of velocity u and excess mass $\rho - \rho_a$, respectively; subscript a refers to the ambient values, and g' corresponds to the mass-based effective gravitational acceleration

For $E = 0$ the structure of the shallow water equations of ET for dRi_E/dx and dH/dx are consistent with the Bresse equations for open channel flows, and the flow becomes critical when Ri_E, or the Froude number $Ri_E^{-1/2}$ is close to one. As noted above, however, the flow scales are different from those of open channel flows. Full consistency can be achieved by adopting the same approach for both flows, i.e., by deriving the depth and velocity scales of gravity currents from the density distribution as well. A suitable set of scales for gravity currents is

$$g' h^2 = 2g \int \frac{\bar{\rho} - \rho_a}{\rho_a} y dy = S_1 \Delta H^2$$

$$g' h^2 = g \int \frac{\bar{\rho} - \rho_a}{\rho_a} dy = S_2 \Delta H$$

$$g' uh = B = \Delta UH \tag{5}$$

where ρ_s = density at the source; g' = mean buoyancy; h = depth; and u = velocity of the dense layer. The excess pressure force and the excess bottom pressure are thus used to define scales g' and h instead of shape factors, and the velocity is derived from the buoyancy flux. When the buoyancy flux is known, the flow scales can be determined without measuring velocities (Bühler et al. 1991). Another advantage of mass-based flow scales is that g' depends on the vertical distribution of buoyancy, whereas Δ would be obtained by fully diluting the flux of buoyancy in the volume flux. By relating the flow scales to the distribution of a dye, they can be used for nonbuoyant shear flows as well (Princevac et al. 2010). For open channel flows $\rho_a = 0$, $\rho = \rho_s$, h is the water depth, and $g' = g$.

Shape coefficients are then required to relate the volume flux and the momentum flux to these flow scales. A suitable choice is

$$\gamma uh = \int \bar{u} dy$$

$$\beta \gamma u^2 h = \int \bar{u}^2 dy \tag{6}$$

where γ modifies the water depth. Experimental data by Altinakar (1993) suggest a range of γ from 1.1 to 1.86 in gravity currents with a mean value of 1.4. The flow can thus be considered as consisting of a dense bottom layer of depth h, superimposed by a layer of thickness $(\gamma - 1)h$ of clear fluid, which flows at the same velocity u. This approach is similar to the one proposed by Escudier and Maxworthy (1973) for thermals, where they invoked the concept of added mass to account for the momentum of clear ambient fluid carried along with these clouds. For open channel flows, β is the momentum coefficient, and $\gamma = 1$. Shape factors for non-Boussinesq flows were derived by Princevac et al. (2009).

The continuity, momentum, and buoyancy equations for gravity currents can then be stated as

$$\frac{d}{dx}(hu) = E^* u \tag{7}$$

$$\frac{d}{dx}\left(\beta \gamma h u^2 + \frac{1}{2} g' h^2 \cos\varphi\right) = g' h \sin\varphi - C_D^* u^2 \tag{8}$$

$$\frac{d}{dx}(g'hu) = 0 \tag{9}$$

where the star denotes mass-based quantities. E^* is now a function of the Richardson number $Ri^* = g'h\cos\varphi/u^2$. By ignoring any variations of φ and the shape constants along x, these relations reduce to

$$\frac{dh}{dx} = \frac{E^*(2\beta\gamma - 1/2\,Ri^*) - Ri^*\tan\varphi + C_D^*}{\beta\gamma - Ri^*} \tag{10}$$

$$\frac{h}{3Ri^*}\frac{dRi^*}{dx} = \frac{E^*(\beta\gamma + 1/2\,Ri^*) - Ri^*\tan\varphi + C_D^*}{\beta\gamma - Ri^*} \tag{11}$$

The flow is again critical with respect to the interfacial long wave speed when the denominators vanish, and Ri^* is of order 1. For $E^* = 0$, $g' = g$, and $\gamma = 1$, (7) to (11) reduce to the shallow water equations for open channel flows. The flow scales of ET for calm ambient waters are related to the mass-based ones by $h = HS_1/S_2$, $g' = \Delta S_2^2/S_1$, $u = U/S_2$, $\beta = S_2$, $\gamma = S_2^2/S_1$, $D^* = D\,S_1/S_2$, $Ri^* = RiS_2^3$, and $C_D^* = C_D S_2^2$.

Altinakar (1993) found all but one value of $\beta = S_2$ between 0.91 and 1.11. Somewhat larger values of 1.01 to 1.23 were reported by Princevac et al. (2009) for katabatic winds. They are in the range of β in open channels or ducts, from which gravity currents may emerge (Chow 1959).

Flows Controlled by Opposing Jets

Wilson (1977) and other investigators conducted experiments to dissipate excess energy in stilling basins. They directed jets against the oncoming flow to create hydraulic jumps. Oehy et al. (2010) applied this concept to internal flows and explored the possibility of backing up turbidity currents in reservoirs by means of opposing submerged jets. They carried out simulations and experiments, which showed that this greatly enhances sedimentation and helps to keep bottom outlets from getting clogged. In the following we shall assume that the slope and the sedimentation over the control section can be neglected, that jets emerge from a number of equidistant nozzles arranged in the spanwise direction, and that they are inclined at an angle θ relative to the bed as shown in Fig. 2. The jets are associated with a flow rate q and a momentum flux m per unit width, regardless of the number of nozzles they emerge from. The jets are thus replaced by an equivalent line source (from a slot) for the purpose of the analysis. The upper layer is considered to be at rest ($u_a = 0$).

The conservation equations for the fluxes of volume, momentum, and buoyancy are

$$\gamma h_1 u_1 + q = \gamma h_2 u_2 \tag{12}$$

$$\frac{1}{2}g_1' h_1^2 + \beta\gamma u_1^2 h_1 - m\cos\theta = \frac{1}{2}g_2' h_2^2 + \beta\gamma u_2^2 h_2 \tag{13}$$

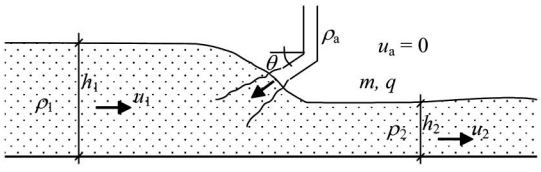

Fig. 2. Jets opposing a flow as, for example, a turbidity current

$$g_1' h_1 u_1 = g_2' h_2 u_2 = B \tag{14}$$

where β and γ are assumed to be equal on both sides of the injection.

With $q_i = \gamma u_i h_i$ we can write $q_1 + q = q_2$. For a convenient presentation in graphs we may redefine $Ri_i = Ri_i^*/(\beta\gamma)$, such that $Ri_i = 1$ for critical flow. The flux $\gamma u_i^2 h_i$ can be expressed as $\{B/(\beta\gamma Ri_i)\}^{1/3} q_i$, which leaves

$$\frac{1}{Ri_1^{1/3}}\left(1 + \frac{1}{2}Ri_1\right) = \frac{q_2}{q_1}\frac{1}{Ri_1^{1/3}}\left(1 + \frac{1}{2}Ri_2\right) + \frac{\gamma^{1/3} m\cos\theta}{q_1(\beta^2 B)^{1/3}} \tag{15}$$

For free surface flows $g' = g$, $\gamma = 1$, and $u_1^2 h_i$ can be expressed as $\{gq_i/(\beta Ri_i)\}^{1/3} q_i$, such that

$$\frac{1}{Ri_1^{1/3}}\left(1 + \frac{1}{2}Ri_1\right) = \left(\frac{q_2}{q_1}\right)^{4/3}\frac{1}{Ri_1^{1/3}}\left(1 + \frac{1}{2}Ri_2\right) + \frac{m\cos\theta}{(\beta^2 g q_1^4)^{1/3}} \tag{16}$$

Solutions can be obtained by substituting $Ri_1 = z^3$ and by denoting the right-hand side of (15) or (16) by r, which leaves $z^3 - 2rz + 2 = 0$. A further substitution of $z = 2(2r/3)^{1/2}\cos\omega$ leads to solutions of the form $\cos(3\omega) = -[3/(2r)]^{3/2}$, such that $\omega = \arccos[-3/(2r)]^{3/2}/3$. Solutions $z = Ri_1^{1/3} = 2(2r/3)^{1/2}\cos\omega$ lead to the subcritical branch in Fig. 3, $z = Ri_1^{1/3} = 2(2r/3)^{1/2}\cos(\omega + 4\pi/3)$ to the supercritical one. An analogous procedure can be used for cases where the downstream flow conditions and Ri_2 are known.

From (15) we obtain for gravity currents

$$\frac{1}{Ri_2^{1/3}}\left(1 + \frac{1}{2}Ri_2\right) = \frac{q_1}{q_2}\frac{1}{Ri_1^{1/3}}\left(1 + \frac{1}{2}Ri_1\right) - \frac{\gamma^{1/3} m\cos\theta}{q_2(\beta^2 B)^{1/3}} \tag{17}$$

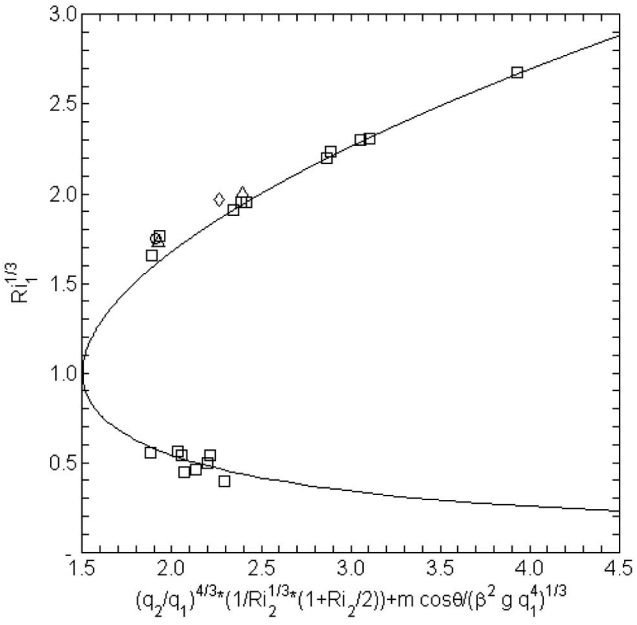

Fig. 3. Relation between downstream conditions and upstream Richardson number Ri_1 [Eq. (16)]; eight 5-mm pipes (squares), four 7.5-mm pipes (circles), eight 10-mm pipes (diamonds), and two 10-mm pipes (triangles)

J. Hydraul. Eng. 2013.139:55-59.

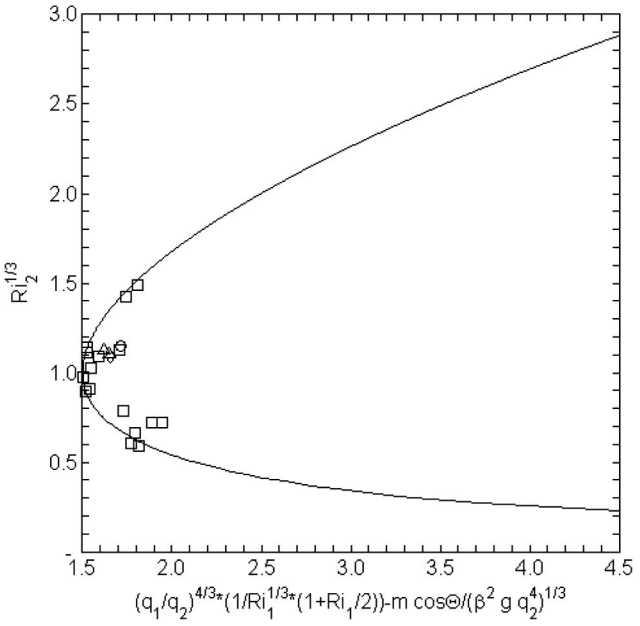

Fig. 4. Relation between upstream conditions and downstream Richardson number Ri_2; symbols as in Fig. 3

The corresponding solution for open channel flows is shown in Fig. 4. For $q_j = m = 0$ and a supercritical flow upstream ($Ri_1 < 1$), the lower branch in this figure denotes the undisturbed throughflow ($Ri_2 = Ri_1$), and the upper branch shows the solution for an arrested hydraulic jump with the conjugate downstream conditions. Relations (15) and (16) as well as the ones for Ri_2 can also be expressed in terms of the more generally used Froude number $F_i = Ri_i^{-1/2}$.

Experiments

The experiments were carried out for open channel flows in a glass-walled flume of 0.4 m width and 0.5 m depth (Fig. 5). The injection angle was $\theta = 15°$. A weir was located 3 m upstream from the injection pipes and allowed for the establishment of supercritical flows within the test section. The upstream and downstream depths were measured by point gauges. Depth measurements were made in cross sections both between and at the spanwise locations of the injection pipes. Values in each cross section were averaged.

Most of the experiments shown in Figs. 3 and 4 were performed with eight equidistant discharge pipes, with one-half the distance left free adjacent to the walls. These pipes had an inner diameter of 5 mm. A few other experiments were made with 7.5 and 10 mm pipes. For the present purpose β was chosen as 1.07 for both the pipe flow and the open channel flow (Chow 1959). The depth h_1 ranged from 0.02 to 0.09 m, u_1 from 0.25 to 1.6 m/s, q from 0.6 to $2.8 \cdot 10^{-3}$ m^2/s, and m from 0.9 to $19.6 \cdot 10^{-3}$m^3/s^2. The agreement with the predictions is quite satisfactory; in particular, there is no clear dependence on the number of pipes used.

In most cases the flow was backed up and subcritical upstream of the pipes, as shown in Figs. 3 and 4, but in some of the experiments the flow remained supercritical everywhere (data on the lower branch of Figs. 4 and 5). Similarly, the flow can be subcritical on both sides of the pipes or on their downstream side only.

Application to Turbidity Currents, An Example

Consider an undisturbed turbidity current in a reservoir flowing along the talweg as sketched in Fig. 2 with a velocity u_0 of 0.6 m/s and having a depth h_0 of 2 m just upstream of the location of the nozzles of the opposing jets. The sediment concentration according to typical turbidity currents is assumed to be 1%, which corresponds to $g_0' = 0.16$ m/s^2, and $B_0 = 0.19$ m^3/s^3. With $\beta = 1.07$ and $\gamma = 1.4$ this corresponds to $Ri_0 = 0.59$, and the flux per unit width is $q_0 = 1.68$ m^2/s. A stream q of 0.05 m^2/s per unit width is available for injection with a momentum of $m = 0.5$ m^3/s^2 at a nozzle inclination of $\theta = 10°$. To what Ri_1 can the upstream flow be backed up? The buoyancy loss in the backed up flow region is estimated at 50%, such that $B_1 = B_2 = 0.096$ m^3/s^3, and if entrainment is neglected, $q_0 = q_1$. The Richardson number on the downstream side can be assumed to be equal to that of the undisturbed current on the same slope, i.e., $Ri_2 = Ri_0$. The factor r according to (15) then assumes a value of 2.27. As the upstream flow cannot be more supercritical than the downstream one, the upper branch in Fig. 3 is relevant, and $Ri_1^{1/3} = 1.85$, or $Ri_1 = 6.33$. The value of $u_1 = [B_1/(Ri_1\beta\gamma)]^{1/3}$ can then be recovered as 0.22 m/s and the depth $h_1 = q_1/\gamma u_1$ as 5.53 m. The total flow depth thus increases from $\gamma h_0 = 2.8$ m to about $\gamma h_1 = 7.74$ m owing to the backup. The determination of the relevant flow parameters is obviously more difficult for these internal flows than for those in a stilling basin. In particular, the buoyancy loss will have to be determined by an iterative procedure by making use of numerical models, such as

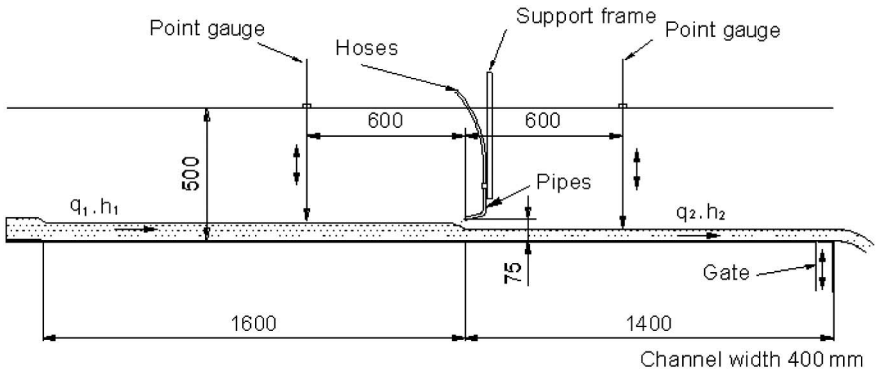

Fig. 5. Experimental arrangement for jets opposing an open channel flow (measurements in mm)

J. Hydraul. Eng. 2013.139:55-59.

ANSYS-CFX12 or FLOW 3D. It should be noted, however, that the jets also help to keep fine sediments in suspension after a turbidity current dies out and during normal operation in turbid reservoirs. In two-layer flows oscillations of a large amplitude may occur when a jet hits a moving interface (Cotel 2010). As the causes are not well understood yet, the jets should emerge from nozzles, which are submerged in the oncoming flow.

Conclusions

Mass-based depth and velocity scales for gravity currents are outlined here. They provide a reliable alternative to conventional scales derived from the velocity distribution and can be used for open channel flows as well. The extent to which turbidity currents and free surface flows can be backed up by jets opposing them is determined. Experiments were carried out for flows with a free surface, and the results agree well with these predictions. An example is provided on jets backing up a turbidity current in a reservoir, a measure that increases its deposition rate before it reaches the dam. The corresponding flow parameters are more difficult to assess than for jumps induced in free surface flows, but such jets also help to keep fine sediment in suspension in turbid reservoirs and after a turbidity current dies out.

Notation

The following symbols are used in this paper:

B = buoyancy flux;
C_D = velocity-based drag coefficient;
C_D^* = mass-based drag coefficient;
E = velocity-based entrainment function;
E^* = mass-based entrainment function;
Fr = Froude number;
g = gravitational acceleration;
g' = effective gravitational accelerations, mass-based;
H = velocity-based flow depth;
h = mass-based flow depth;
m = momentum flux per unit width from nozzles;
q = volume flux from nozzles, per unit width;
q_i = volume flux per unit width in main flow;
Ri = modified Richardson number;
Ri_E = velocity-based Richardson number;
Ri^* = mass-based Richardson number;
S_1, S_2 = shape factors;
U = velocity-based average flow velocity;
u = mass-based average flow velocity;
$\bar{u}$ = local fluid velocity;
u_a = velocity of ambient fluid;
x = coordinate along the slope;
y = coordinate transverse to the slope;
β = momentum coefficient;
γ = factor modifying depth of gravity currents;
Δ = effective gravitational acceleration, velocity based;
θ = inclination angle of nozzles;
$\bar{\boldsymbol{\rho}}$ = local fluid density;
ρ_a = density of ambient fluid;
ρ_s = density at the source; and
φ = slope angle.

Subscripts in (12) to (17)

0 = in the undisturbed turbidity current;
1 = in the upstream flow; and
2 = in the downstream flow.

References

Altinakar, M. S. (1993). "Weakly depositing turbidity currents on small slopes." Ph.D. thesis no. 738, Dept. of Civil Engineering, Ecole Polytechnique Fédérale de Lausanne (EPFL), Lausanne, Switzerland.

Bühler, J., Wright, S. J., and Kim, Y. (1991). "Gravity currents advancing into a coflowing fluid." *J. Hydraul. Res.*, 29(2), 243–257.

Chow, V.-T. (1959). *Open channel hydraulics*, McGraw-Hill, New York.

Cotel, A. J. (2010). "A review of recent developments on turbulent entrainment in stratified flows." *Phys. Scr.*, T142, 014044:1–014044:4.

Ellison, T. H., and Turner, J. S. (1959). "Turbulent entrainment in stratified flows." *J. Fluid Mech.*, 6(3), 423–448.

Escudier, M. P., and Maxworthy, T. (1973). "On the motion of turbulent thermals." *J. Fluid Mech.*, 61(3), 541.

France, P. W. (1981). "An investigation of a jet-assisted hydraulic jump." *J. Hydraul. Res.*, 19(4), 325–337.

Hager, W. H. (1992). *Energy dissipators and hydraulic jump.*, Kluwer, Dordrecht.

Morton, B. R., Taylor, G. I., and Turner, J. S. (1956). "Turbulent gravitational convection from maintained and instantaneous sources." *Proc. R. Soc., A*, 234(1196), 1–23.

Oehy, C. D., De Cesare, G., and Schleiss, A. J. (2010). "Effect of inclined jet screen on turbidity current." *J. Hydraul. Res.*, 48(1), 81–90.

Oehy, C. D., and Schleiss, A. J. (2003). "Physical and numerical modelling of a turbidity current flowing through a permeable screen." *Proc., 30th IAHR Congress*, J. Ganoulis, and P. Prinos, eds., Thessaloniki, Greece, Theme C, Vol. 1, 397–404.

Prandtl, L. (1926). "Ueber die ausgebildete Turbulenz." *Proc., 2nd Int. Congr. for Appl. Mech.*, E. Meissner, ed., Füssli, Zurich, 62–74.

Princevac, M., Bühler, J., and Schleiss, A. J. (2009). "Mass-based depth and velocity scales for gravity currents and related flows." *Environ. Fluid Mech.*, 9(4), 369–387.

Princevac, M., Bühler, J., and Schleiss, A. J. (2010). "Alternative depth-averaged models for gravity currents and free shear flows." *Environ. Fluid Mech.*, 10(3), 369–386.

Sequeiros, O. E., Cantero, M. I., and Garcia, M. H. (2009). "Sediment management by jets and turbidity currents with application to a reservoir for flood and pollution control in Chicago, Illinois." *J. Hydraul. Res.*, 47(3), 340–348.

Tople, S. K. P., Porey, P. D., and Ranga Raju, K. G. (1986). "Hydraulic jump under the influence of two-dimensional cross jets." *J. Inst. Eng. Civ. Eng. Div. (India)*, 66(6), 277–283.

Wilson, E. H. (1977). "Stabilization of the hydraulic jump by jets." *Water Power Dam Constr.*, 29(3), 40–45.

Wright, S. J. (1994). "The effect of ambient turbulence on jet mixing." *Recent research advances in the fluid mechanics of turbulent jets and plumes*, NATO ASI Series, Kluwer, Dordrecht, 13–27.

J. Hydraul. Eng. 2013.139:55-59.